Curve Subdivision in SE(2)

Jan Hakenberg, ETH Zürich
2018-07-26

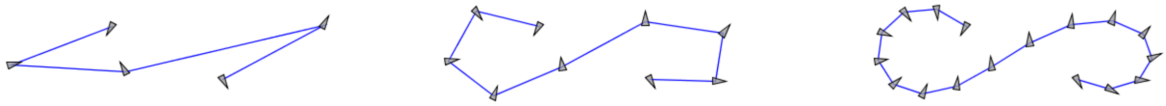

Figure: A point in the special Euclidean group SE(2) consists of a position in the plane and a heading. The figure shows two rounds of cubic B-spline subdivision of an initial sequence of five control points in SE(2). A point is indicated by an arrowhead. ■

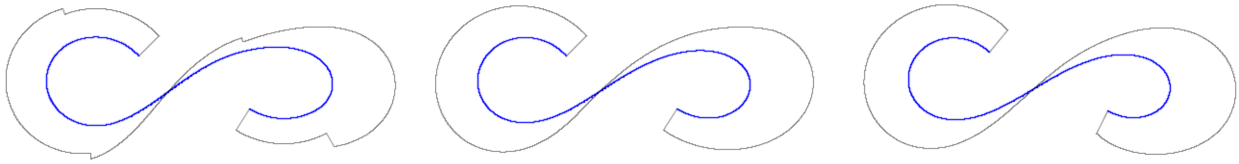

Figure: Limit curves projected to the plane (blue) with curvature comb generated by quadratic, cubic, and quartic B-spline refinement of the initial sequence of five control points in SE(2). ■

Abstract: We demonstrate that curve subdivision in the special Euclidean group SE(2) allows the design of planar curves with favorable curvature. We state the non-linear formula to position a point along a geodesic in SE(2). Curve subdivision in the Lie group consists of trigonometric functions. When projected to the plane, the refinement method reproduces circles and straight lines. The limit curves are designed by intuitive placement of control points in SE(2).

Keywords: non-linear curve subdivision, smooth refinement, curvature, special Euclidean group, Dubins path

Introduction

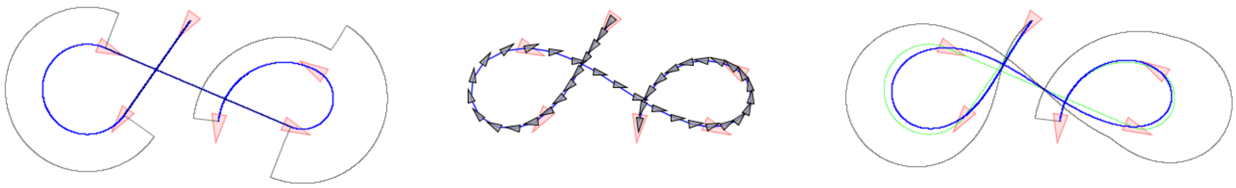

Figure: In a Dubins path the heading of a control point in SE(2) matches the tangent of the curve. The curvature of the Dubins path is generally discontinuous as indicated by the curvature comb. The center image shows the refined sequence after 3 rounds of cubic B-spline subdivision in SE(2). To the right is the limit curve with continuous curvature. ■

The general purpose of curve subdivision schemes is the design of curves from efficient and intuitive user input. The characteristics of limit curves generated by *linear* subdivision rules are well-understood. Linear schemes produce smooth curves, yet they don't distribute the curvature well.

Figure: Left, limit curve with curvature comb generated by traditional cubic B-spline subdivision with control points in $\mathbb{R}^2$. Right, the non-linear interpolatory scheme by [2005 Malcolm A. Sabin, Neil A. Dodgson] inserts a point by fitting circles through adjacent control points and averaging their radii. The image shows the limit curve generated from three initial control points. The curvature is not smooth. ■

In the field of robotics, the Lie group SE(2) is used to model the pose of a car-like mobile robot that moves in the plane. A point $p = (x, y, \theta) \in \mathrm{SE}(2)$ encodes the position $(x, y) \in \mathbb{R}^2$ in the plane with heading $\theta \in [-\pi, \pi)$.

The scheme that we detail in this article is based on refinement along geodesics in SE(2). A geodesic in SE(2) is either a circle or a straight line when projected to the plane.

We provide evidence that the proposed refinement scheme when applied to the control points of a Dubins path generally results in a trajectory with improved curvature while remaining fairly close to the original path. We also motivate the applicability of the scheme for the design of appealing planar curves.

Curve subdivision in manifolds

[2014 Nira Dyn, Nir Sharon] formulate curve subdivision in a manifold with metric using geodesics. We restate their approach in a slightly modified notation.

Let M be a manifold with metric. Between two sufficiently close points $p, q \in M$ with $p \neq q$ a unique shortest path $\tau_{p,q} : \mathbb{R} \to M$ exists with parameterization proportional to arc-length and $\tau_{p,q}(0) = p$, and $\tau_{p,q}(1) = q$. We refer to $\tau_{p,q}$ as the *geodesic* that connects p and q. For all $p \in M$, we define $\tau_{p,p}(\lambda) := p$ for all $\lambda \in \mathbb{R}$. For enhanced readability, when refering to $\tau_{p,q}$, we assume that the points $p, q \in M$ are sufficiently close so that the geodesic $\tau_{p,q}$ is well-defined and unique.

Higher-order subdivision requires nested averaging. We define the short-hand $[p, q]_\lambda := \tau_{p,q}(\lambda)$. The shortest path from p to q is the same as the shortest path from q to p reversed: The relation $[p, q]_\lambda = [q, p]_{1-\lambda}$ holds for all $p, q \in M$ and $\lambda \in \mathbb{R}$. In particular, $[p, q]_{1/2} = [q, p]_{1/2}$.

In all examples that we consider, the manifold is a Lie group $(M, .)$ with geodesics of the form

$$[p, q]_\lambda = p.\exp\left(\lambda \log\left(p^{-1}.q\right)\right) \qquad \text{for all } p, q \in M \text{ and } \lambda \in \mathbb{R}.$$

Example: Consider the 3D rotation group $M = SO(3)$. An element $p \in SO(3)$ is a 3×3 orthogonal matrix with determinant +1. The group action is matrix multiplication. The matrix logarithm maps to the vector space of skew-symmetric 3×3 matrices. An implementation of the logarithm is stated in [2009 Gregory Chirikjian]. The matrix exponential is obtained using [1815 Olinde Rodrigues] formula. ∎

Example: Consider the Euclidean vector space as Lie group $(\mathbb{R}^n, +)$. The functions $\exp = \log = \mathrm{Id}$. Given vectors $p, q \in \mathbb{R}^n$, the geodesic expression simplifies to the parameterization of a straight line

$$[p, q]_\lambda = p + \lambda(q - p) \qquad \text{for all } p, q \in M \text{ and } \lambda \in \mathbb{R}. \ ∎$$

Refinement along geodesics

Linear B-spline subdivision inserts the point $[p, q]_{1/2}$ in the center of the shortest path between two control points $p, q \in M$.

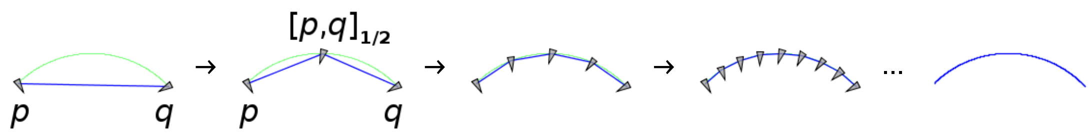

Figure: Insertion of the point $[p, q]_{1/2}$ along the geodesic between $p, q \in M$. The insertion is repeated for every new edge ad infinitum. ∎

Quadratic B-spline subdivision replaces two adjacent control points $p, q \in M$ with the pair $[p, q]_{1/4}$ and $[p, q]_{3/4}$.

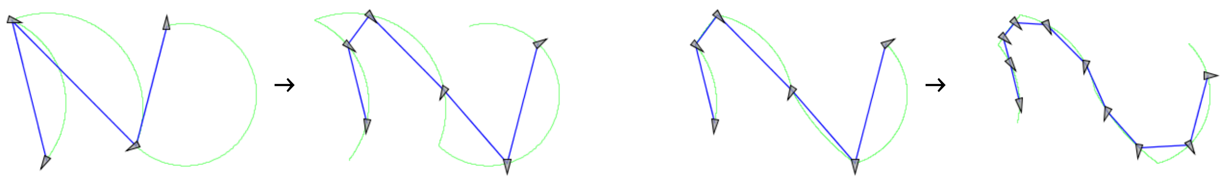

Figure: Two rounds of subdivision starting with a sequence of four control points in SE(2). The quadratic B-spline rule inserts two control points at ratios 1/4 and 3/4 along each geodesic segment in green. ∎

Cubic B-spline subdivision has the insertion rule identical to linear B-spline subdivision. The mask to reposition a point q in the control point sequence (p, q, r) with $p, q, r \in M$ is $\tilde{q} = [[p, q]_{3/4}, [q, r]_{1/4}]_{1/2}$.

In case of the Euclidean vector space $(\mathbb{R}^n, +)$ the formula simplifies to the well-known linear combination

$$\tilde{q} = \left[\tfrac{1}{4}p + \tfrac{3}{4}q,\ \tfrac{3}{4}q + \tfrac{1}{4}r\right]_{1/2} = \tfrac{1}{8}p + \tfrac{3}{4}q + \tfrac{1}{8}r$$

Quartic B-spline subdivision operates on triples (p, q, r) with $p, q, r \in M$ for which the center point q is substituted by two new points

$$[[p, q]_{3/8}, [q, r]_{1/8}]_{1/2} \quad \text{and} \quad [[r, q]_{3/8}, [q, p]_{1/8}]_{1/2}$$

In case of the interpolatory four-point scheme with tension parameter $\omega = 1/16$, the mask to insert a point $m \in M$ in the "center" of the control point sequence (p, q, r, s) with $p, q, r, s \in M$ is

$$m = [[p, q]_{9/8}, [r, s]_{-1/8}]_{1/2}$$

[2014 Nira Dyn, Nir Sharon • Example 5.2] states refinement and convergence also for the interpolatory 6-point scheme by [1989 Gilles Deslauriers, Serge Dubuc].

Refinement in SE(2)

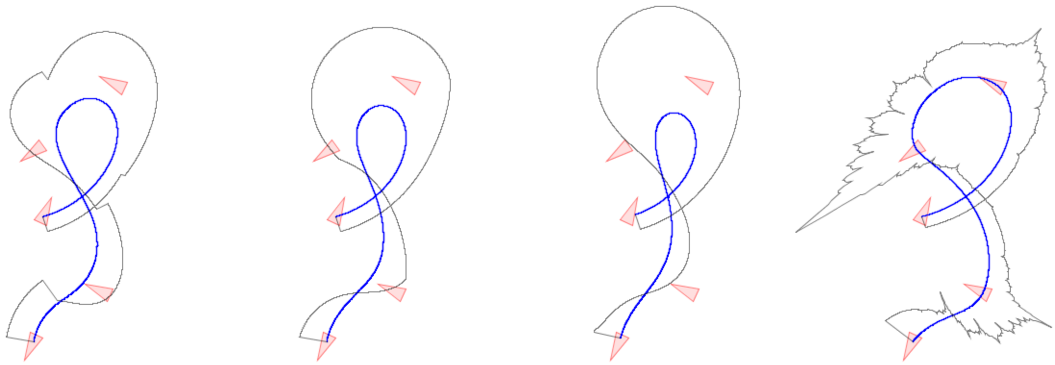

Figure: Limit curves and curvature generated by refinement of a sequence of five control points in SE(2) with B-spline rules of order 2–4 as well as the interpolatory 4-point scheme with tensor parameter ω=1/16. ■

SE (2) denotes the special Euclidean group. The 3-dimensional Lie group consists of all affine rigid transformations of $\mathbb{R}^2$. An element in the group is typically encoded as a 3×3 matrix of the form

$$m = \begin{pmatrix} \mathrm{Cos}[\theta] & -\mathrm{Sin}[\theta] & x \\ \mathrm{Sin}[\theta] & \mathrm{Cos}[\theta] & y \\ 0 & 0 & 1 \end{pmatrix}$$

The group action is matrix multiplication. The angles θ and $\theta + 2\pi$ yield the same matrix m. We parameterize the group elements using triples of the form (x, y, θ) for $x, y \in \mathbb{R}$ and $\theta \in [-\pi, \pi)$. The neutral element of the group is at (0, 0, 0).

We wish to perform curve subdivision in the covering group $M = \overline{\mathrm{SE}}(2)$ to account for winding numbers. Angular components with winding number give more freedom in the design of curves. The coordinate of a point in $\overline{\mathrm{SE}}(2)$ is a triple of the form (x, y, θ) with $x, y, \theta \in \mathbb{R}$. The group action and inverse of points in $\overline{\mathrm{SE}}(2)$ in triple notation are derived from matrix multiplication and matrix inversion as

```
SE2CoveringCombine[{px_, py_, pθ_}, {qx_, qy_, qθ_}] :=
  {px + qx Cos[pθ] - qy Sin[pθ], py + qy Cos[pθ] + qx Sin[pθ], pθ + qθ}
```

```
SE2CoveringInverse[{x_, y_, θ_}] := {-x Cos[θ] - y Sin[θ], x Sin[θ] - y Cos[θ], -θ}
```

The logarithm maps a point in the Lie group that is sufficiently close to the neural element into the tangent space at the neural element. The tangent space is the Lie algebra. The function $\log : D \subset \overline{\mathrm{SE}}(2) \to \mathfrak{se}(2)$ is derived from the matrix logarithm as

```
SE2Log[{x_, y_, θ_}] := {θ/2 (y + x Cot[θ/2]), θ/2 (-x + y Cot[θ/2]), θ}
SE2Log[{x_, y_, θ_}] := {x, y, 0} /; θ == 0
```

The exponential maps a vector from the Lie algebra to the Lie group. The function $\exp : \mathfrak{se}(2) \to \overline{\mathrm{SE}}(2)$ is derived from the matrix exponential as

```
SE2Exp[{u_, v_, ω_}] := {(v (Cos[ω] - 1) + u Sin[ω])/ω, (-u (-1 + Cos[ω]) + v Sin[ω])/ω, ω}
SE2Exp[{u_, v_, ω_}] := {u, v, 0} /; ω == 0
```

The term $[p, q]_\lambda = p.\exp(\lambda \log(p^{-1}.q))$ is a combination of the above functions. The point $[p, q]_\lambda \in \overline{\mathrm{SE}}(2)$ is computed as

```
SE2Split[p_, q_, λ_] :=
 SE2CoveringCombine[p, SE2Exp[λ SE2Log[SE2CoveringCombine[SE2CoveringInverse[p], q]]]]
```

Example: Let $p = (1, 2, 3)$, $q = (4, 5, 6)$ in $\overline{\mathrm{SE}}(2)$ and $\lambda = 0.7$. Then, $[p, q]_\lambda = \{4.48383 \ldots, 3.21435 \ldots, 5.1\}$. ■

Lemma 1: Let $\tau_\alpha : \overline{\mathrm{SE}}(2) \to \overline{\mathrm{SE}}(2)$ be defined as $(x, y, \theta) \mapsto (x, y, \theta + \alpha)$. Then, $\tau_\alpha([p, q]_\lambda) = [\tau_\alpha(p), \tau_\alpha(q)]_\lambda$ for all $\alpha \in \mathbb{R}$. *Proof:*

```
SE2Split[{px, py, pθ}, {qx, qy, qθ}, λ] + {0, 0, α} ==
  SE2Split[{px, py, pθ + α}, {qx, qy, qθ + α}, λ] // Simplify
```

```
True
```

Generally, the logarithm is not well-defined for all points in the Lie group. Due to $[p, q]_\lambda = p.[0, p^{-1}.q]_\lambda$ it is sufficient to investigate the expression for geodesics that start in the origin $[0, r]_\lambda = \exp(\lambda \log(r))$ for $r \in \overline{\mathrm{SE}}(2)$ and $\lambda \in \mathbb{R}$.

```
SE2Split[{0, 0, 0}, {x, y, θ}, λ] // Simplify
```

$$\left\{\mathrm{Csc}\left[\frac{\theta}{2}\right] \mathrm{Sin}\left[\frac{\theta \lambda}{2}\right] \left(x \,\mathrm{Cos}\left[\frac{1}{2} (\theta - \theta \lambda)\right] + y \,\mathrm{Sin}\left[\frac{1}{2} (\theta - \theta \lambda)\right]\right), \mathrm{Csc}\left[\frac{\theta}{2}\right] \mathrm{Sin}\left[\frac{\theta \lambda}{2}\right] \left(y \,\mathrm{Cos}\left[\frac{1}{2} (\theta - \theta \lambda)\right] - x \,\mathrm{Sin}\left[\frac{1}{2} (\theta - \theta \lambda)\right]\right), \theta \lambda\right\}$$

The logarithm function includes the cotangent function that has poles. The poles of $\csc[\theta/2] = 1/\sin[\theta/2]$ are at $\theta = n 2\pi$ for all integers $n \in \mathbb{Z}$. In case $n = 0$, i.e. $\theta = 0$, the term is well defined because

```
Limit[Csc[θ / 2] Sin[θ λ / 2], θ → 0]
```

```
λ
```

For the angle $\theta = 0$, the geodesic $[0, (x, y, 0)]_\lambda = (\lambda x, \lambda y, 0)$ with $\lambda \in \mathbb{R}$ is a straight line in $\overline{\mathrm{SE}}(2)$. For angles of the form $\theta = n 2\pi$ with non-zero integer $n \in \mathbb{Z}\backslash\{0\}$ the geodesic is a circle with infinite radius and winding number n. To avoid the singularity in the process of subdivision, two adjacent control points $p, q \in \overline{\mathrm{SE}}(2)$ should not differ in heading by a non-zero multiple of 2π. Finite rounds of subdivision determine if this criterion is satisfied because the heading of two adjacent points contracts according to linear subdivision rules.

In combination with any of the traditional refinement procedures that we stated in the introduction, the formula for $[p, q]_\lambda$ defines curve subdivision in $\overline{\mathrm{SE}}(2)$. The limit curve in $\overline{\mathrm{SE}}(2)$ may be projected to $\mathbb{R}^2$ via $\psi : \overline{\mathrm{SE}}(2) \to \mathbb{R}^2$ with $(x, y, \theta) \mapsto (x, y)$. The projection ψ simply drops the angular component. The projection to Euclidean space $\mathbb{R}^2$ allows to investigate the curvature of the resulting limit curve.

If all points from the input sequence in SE(2) have identical angular component, the projected limit curve equals the limit curve produced by the conventional scheme in $\mathbb{R}^2$.

Corollary: Lemma 1 implies $\psi([p, q]_\lambda) = \psi([\tau_\alpha(p), \tau_\alpha(q)]_\lambda)$ for all angular offsets $\alpha \in \mathbb{R}$. ■

Examples

The paths by [1957 Lester Dubins] form a subset of trajectories in SE(2) that are used in the motion planning for car-like robots. A *Dubins path* is a concatenation of geodesic segments between a given sequence of control points $p_1, \ldots, p_N \in \mathrm{SE}(2)$ so that the normal of the curve transitions continuously in every control point. The curvature is constant along each segment, but generally discontinuous/not defined at the control points. However, if the curvature of the segments is sufficiently bounded, the Dubins path can be executed by a car-like robot.

Three demonstrations below illustrate the smoothing of Dubins paths using curve subdivision in $\overline{\mathrm{SE}}(2)$. The green line indicates the Dubins path defined by initial control points that are indicated as arrowheads in red.

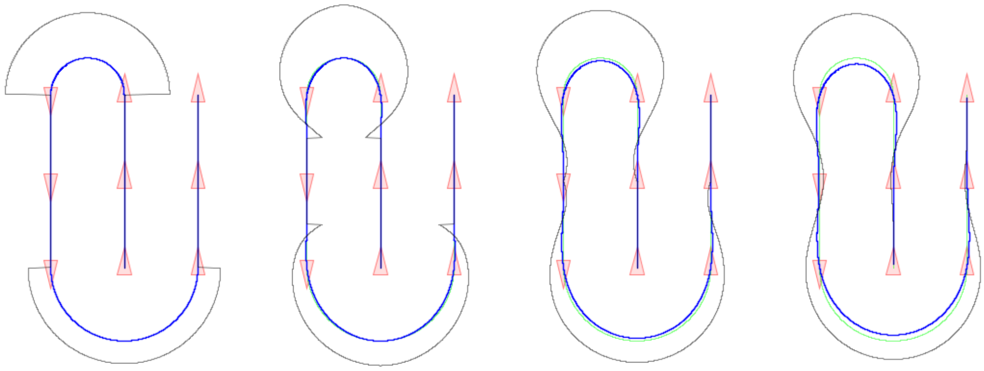

Figure: B-spline refinement of order 1–4 of a Dubins path consisting of two U-turns with different radii. The curvature comb of the limit curve projected to $\mathbb{R}^2$ does not indicate many inflection points when transitioning between a circle and a straight line. ■

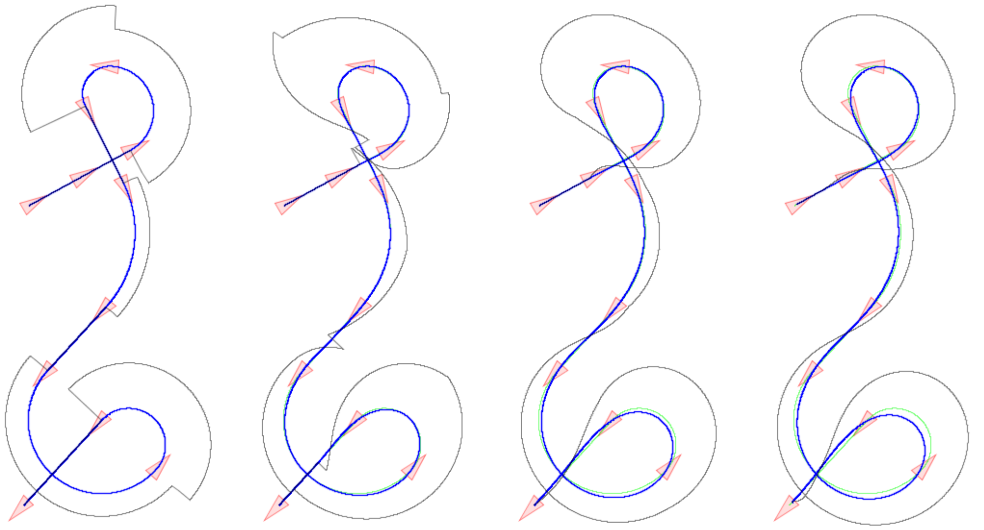

Figure: B-spline refinement of order 1–4 applied to an arbitrary Dubins path. ■

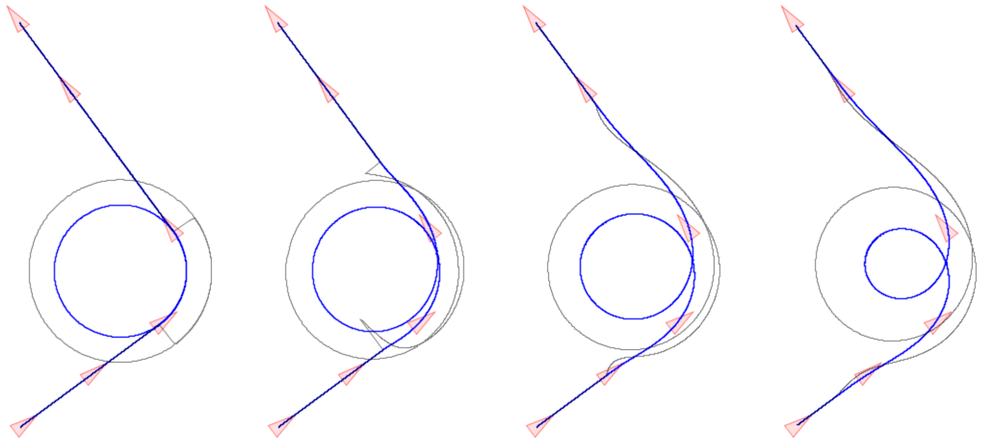

Figure: B-spline refinement of order 1–4 applied to a Dubins path that is almost, but not quite, entirely unlike a 90° turn. The angular difference between the 3rd and 4th control point is $2\pi + \pi/2$. ■

Finally, we make input to curve subdivision control points in $\overline{\mathrm{SE}}(2)$ that do not originate from a Dubins path.

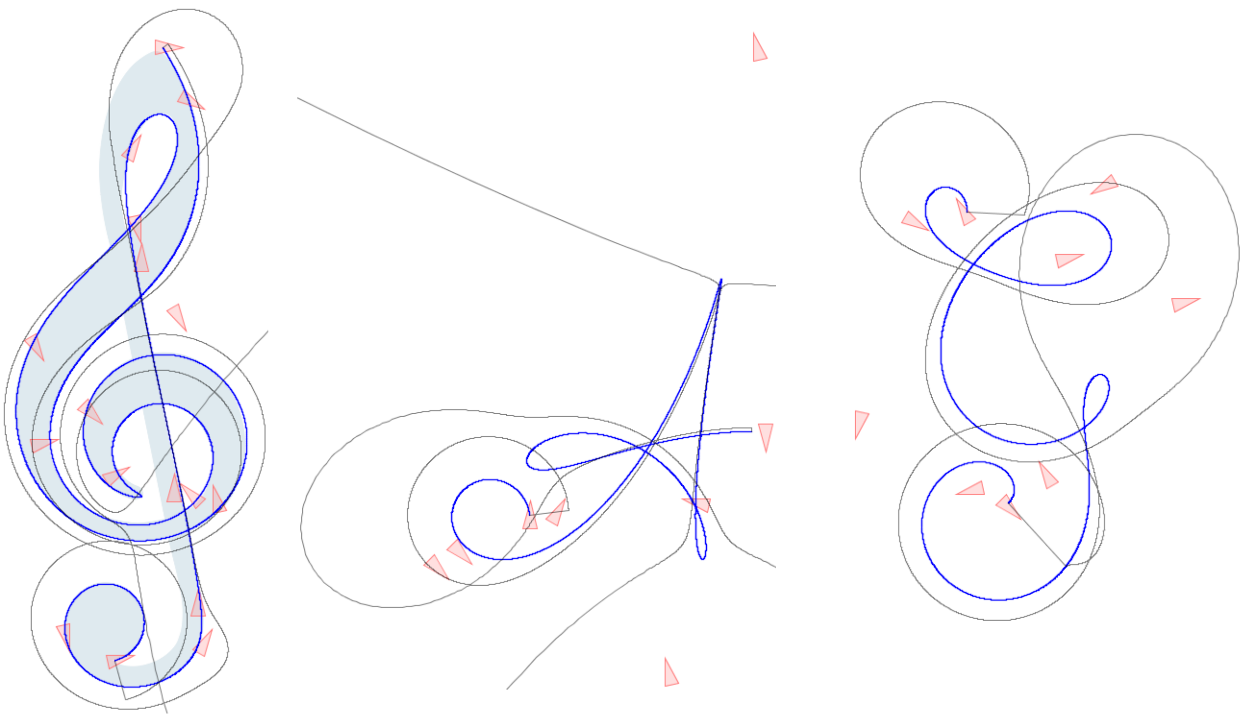

Figure: Cubic B-spline refinement applied to 17 control points to partially contour a treble clef. Quartic B-spline refinement applied to 8 control points to form the letter ‘A’, and 9 control points to form the letter ‘G’. ■

Conclusion

[2007 J. Wallner, E. Nava Yazdani, P. Grohs] state that the log-exponential subdivision on Lie group valued data “essentially has the same properties regarding C1 and C2 smoothness as the linear schemes they are derived from”. For instance, the interpolatory 4-point scheme with tension parameter $0 < \omega < 0.19273 \ldots$ generates C^1 limit curves, see [2009 Jochen Hechler, Bernhard Mößner, Ulrich Reif]. This equivalence may be the reason that curve subdivision schemes have not been investigated for specific Lie groups. Subdivision based on geodesics in $\overline{\mathrm{SE}}(2)$ has the same smoothness properties as the underlying scheme.

Curve subdivision in $\overline{\mathrm{SE}}(2)$ distributes the curvature more regularly along the limit curve than the underlying *linear* scheme in $\mathbb{R}^2$. This roundness effect is due to the influence of the angular component of the control points in the non-linear refinement formula.

The implementation of curve subdivision in $\overline{\mathrm{SE}}(2)$ is numerically efficient and stable. The illustrations in the article were produced by our open-source code [2018 IDSC-Frazzoli].

Future research may quantify how much the limit curve of subdivision in $\overline{\mathrm{SE}}(2)$ deviates from a Dubins path in position and curvature.

References

1815 Olinde Rodrigues: https://en.wikipedia.org/wiki/Rodrigues%27_rotation_formula
1957 Lester Dubins, Dubins path https://en.wikipedia.org/wiki/Dubins_path
1989 Gilles Deslauriers, Serge Dubuc: *Symmetric iterative interpolation processes*
2005 Malcolm A. Sabin, Neil A. Dodgson: *A Circle-Preserving Variant of the Four-Point Subdivision Scheme*
2007 J. Wallner, E. Nava Yazdani, P. Grohs: *Smoothness properties of Lie group subdivision schemes*
2009 Gregory Chirikjian: *Stochastic Models, Information Theory, and Lie Groups*
2009 Jochen Hechler, Bernhard Mößner, Ulrich Reif: C1-Continuity of the generalized four-point scheme
2014 Nira Dyn, Nir Sharon: *Manifold-valued subdivision schemes based on geodesic inductive averaging*
2015 Jan Hakenberg: Curve Subdivision on Riemannian Manifolds - Several Examples
2018 IDSC-Frazzoli: Library for motion planning in Java; https://github.com/idsc-frazzoli/owl